

Effective conjugation and Raman intensities in oligo(para-phenylene)s: A microscopic view from first-principles calculations

Georg Heimel, Dieter Somitsch, Peter Knoll, Jean-Luc Brédas, and Egbert Zojer

Citation: *J. Chem. Phys.* **122**, 114511 (2005); doi: 10.1063/1.1867355

View online: <http://dx.doi.org/10.1063/1.1867355>

View Table of Contents: <http://jcp.aip.org/resource/1/JCPSA6/v122/i11>

Published by the [American Institute of Physics](#).

Additional information on *J. Chem. Phys.*

Journal Homepage: <http://jcp.aip.org/>

Journal Information: http://jcp.aip.org/about/about_the_journal

Top downloads: http://jcp.aip.org/features/most_downloaded

Information for Authors: <http://jcp.aip.org/authors>

ADVERTISEMENT



**ALL THE PHYSICS
OUTSIDE OF
YOUR JOURNALS.**

www.physics-today.org
**physics
today**

Effective conjugation and Raman intensities in oligo(*para*-phenylene)s: A microscopic view from first-principles calculations

Georg Heimel^{a)}

School of Chemistry and Biochemistry, Georgia Institute of Technology, Atlanta, Georgia 30332-0400 and
Institute of Solid State Physics, Graz University of Technology, Petersgasse 16, A-8010 Graz,
Austria

Dieter Somitsch and Peter Knoll

Institute of Experimental Physics, University of Graz, Universitätsplatz 5, A-8010 Graz, Austria

Jean-Luc Brédas

School of Chemistry and Biochemistry, Georgia Institute of Technology, Atlanta, Georgia 30332-0400

Egbert Zojer

Institute of Solid State Physics, Graz University of Technology, Petersgasse 16, A-8010 Graz, Austria and
School of Chemistry and Biochemistry, Georgia Institute of Technology, Atlanta,
Georgia 30332-0400

(Received 8 September 2004; accepted 14 January 2005; published online 23 March 2005)

Electron-phonon coupling in oligo(*para*-phenylene)s is addressed in terms of the off-resonance Raman intensities of two distinct modes at 1220 and 1280 cm^{-1} . On the basis of Albrecht's theory, vibrational coupling and Raman intensities are calculated from *first-principles* quantum-chemical methods. A few-state model is used to evaluate the dependence of the mode intensities on oligomer length, planarity, and excitation wavelength. The link between electron delocalization/conjugation and Raman intensities is highlighted. Extending on prior studies, the present work focuses on providing an in-depth understanding of the origin of this correlation in addition to reproducing experimental findings. The model applied here allows us to interpret the results on a microscopic, quantum-mechanical basis and to relate the observed trends to the molecular orbital structure and nature of the excited states in this class of materials. We find quantitative agreement between the results of the calculations and those of measurements performed on oligo(*para*-phenylene)s of various chain lengths in the solid state and in solution. © 2005 American Institute of Physics. [DOI: 10.1063/1.1867355]

I. INTRODUCTION

Over the past three decades, the field of conjugated polymers has attracted ever increasing attention. Very much like poly(acetylene) is the standard example for a degenerate ground-state system, poly(*para*-phenylene) (PPP) can be seen as the prototypical nondegenerate ground-state material.^{1,2} In addition to exhibiting metallic conductivity when heavily doped,³ PPP and its planarized derivatives have been extensively studied for their optoelectronic properties.^{4–6} The corresponding oligomers, the oligo(*para*-phenylene)s (OPPs), are also of interest: *p*-terphenyl (P3P) and *p*-quaterphenyl (P4P) are used as UV laser dyes,^{7,8} in scintillation counters,⁹ and as wavelength shifters,¹⁰ while the longer *p*-sexiphenyl (P6P) is used as active layer in organic light emitting devices.^{11,12} Moreover, P4P, *p*-quinquephenyl (P5P), and P6P have been exploited in organic field-effect transistors.¹³ Biphenyl (2P) can be viewed as the simplest model compound for this class of materials.

The vibrational spectra of PPP and its planarized derivatives have been the subject of numerous theoretical^{14–16} and experimental investigations.^{17,18} Particular interest was given

to the Raman and resonant Raman spectra of pristine^{19–21} and doped PPP,^{22–24} since these yield important information on the mechanism of electron-phonon coupling in the material. The coupling between electronic and vibrational degrees of freedom strongly affects the nature of the photoexcitations in these materials. Thus, a fundamental understanding of this mechanism can help to optimize the photophysical properties for potential applications.

There are three predominant features in the Raman spectrum of the polymer, at 1220, 1280, and around 1600 cm^{-1} . They have been assigned to totally symmetric ($A_{(g)}$) C–H in-plane bend, C–C inter-ring stretch (see Fig. 1), and aromatic C=C on-ring stretch modes, respectively. These three modes are also present in the oligomers, where the band around 1600 cm^{-1} splits into a doublet which has been assigned to a Fermi-dyad between a fundamental and a combination band. This doublet has been shown to be very sensitive to the effective conjugation length of the OPPs.²⁵

The intensity ratio I_{1280}/I_{1220} was also found to be a good indication for the extension of the conjugated segments in *para*-phenylene oligo- and polymers^{14,26} and has subsequently been used to monitor the quality of synthetic routes for PPP.^{17,27} We note that increasing the conjugation length leads to a decrease of the I_{1280}/I_{1220} ratio; in addition,

^{a)}Electronic mail: georg.heimel@chemistry.gatech.edu

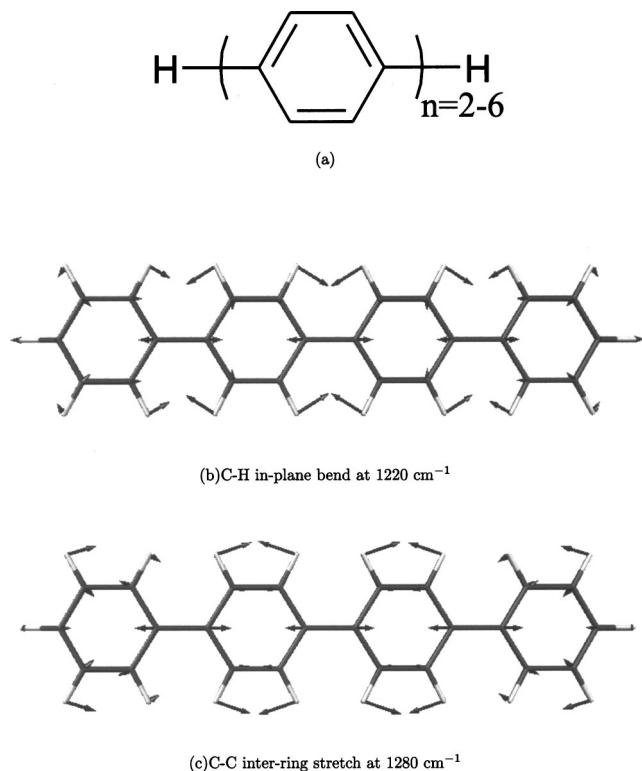


FIG. 1. Molecular structure of the oligo(*para*-phenylene)s (a), atomic displacement patterns calculated for *p*-quaterphenyl at the DFT (mPWLYP/4-31G**) level for the C–H in-plane bend mode at 1220 cm^{-1} (b), and the C–C interring stretch mode at 1280 cm^{-1} (c).

I_{1280}/I_{1220} was observed to decrease upon increasing the laser energy towards the resonant regime.^{18,26,28} It has also been suggested that the I_{1280}/I_{1220} ratio decreases upon planarization of the oligomers.^{28–30}

The goal of the present study is to provide a comprehensive description of the conjugation dependence of the off-resonance Raman intensities of the two modes at 1220 and 1280 cm^{-1} in OPPs containing from two to six phenylene rings (2P–P6P). Rather than simply reproducing the experimentally observed trends, the present work aims at shedding light on the coupling between the vibrational degrees of freedom and the molecular orbital structure and excited states of the OPPs. To that end, we calculated the dependence of I_{1280}/I_{1220} on chain length, planarity, and wavelength by applying quantum-chemical *first-principles* methods on the basis of Albrecht's theory. Our results quantitatively reproduce all the experimental observations mentioned above as well as those described in the present work and allow to trace them down to their microscopic, quantum-mechanical origin.

II. METHODOLOGY

A. Experimental

2P and P4P were purchased from Fluka, P3P from Aldrich and P6P from Tokyo Kasei Kogyo Co. Ltd. All chemicals were of >99% purity and used without further processing. Raman spectra were recorded for polycrystalline powders and, in the case of P3P, also in CH_2Cl_2 solution with a Dilor OMARS 89 triple spectrometer in standard backscattering configuration. Unless otherwise noted, the red

647.1 nm line of a Krypton ion laser (Coherent Innova 90) was used. Incident laser light was collimated to a $\sim 2 \times 0.05$ mm line focus; scattered light was focused onto the 150 μm entrance slit of the spectrometer, yielding a total error of no more than $\pm 1 \text{ cm}^{-1}$ on the Raman frequencies. The signal was detected with a liquid nitrogen cooled charge-coupled device (Wright Instruments). All spectra were recorded with the scanning multichannel technique³¹ and corrected for the spectral sensitivity of the setup. All shown experimental Raman spectra have been normalized to the 1280 cm^{-1} mode.

B. Computational

A number of quantum-chemical program packages allow for the calculation of Raman intensities from static polarizabilities.³² Results from these calculations are often in good agreement with the experimental Raman spectra of the OPPs and their evolution with chain length and planarity.^{33–35} However, this type of calculation is not always optimal for understanding the underlying physics and the microscopic, quantum-mechanical mechanisms that lead to the Raman intensity of a specific mode. Moreover, the incident laser wavelength cannot be taken into account explicitly. Many theoretical models have been developed to describe the Raman spectra of conjugated polymers and oligomers, yielding valuable insight into their vibrational properties.^{15,19,36–41} However, most of them are restricted to the resonant regime, where only coupling to the lowest energy optically allowed excited electronic state needs to be taken into account and higher excited states can safely be neglected. Among these models, the *Ja* mode model developed by Zerbi and co-workers¹⁹ has received a lot of attention in the literature. Therefore, it will later be briefly compared to the model employed in the present work.

In order to access the off-resonance regime and to derive the Raman intensities from readily interpretable quantities, we chose to calculate the scattering cross sections within Albrecht's theory.^{42,43}

The total scattered light intensity I_{if} for a process that promotes a system, e.g., a molecule, from its initial state $|\Psi_i\rangle$ into a final state $|\Psi_f\rangle$ is given by

$$I_{if} \propto (\omega_0 - \omega_{if})^4 \sum_{\rho, \sigma=1}^3 |\langle \Psi_f | \hat{\alpha}_{\rho\sigma} | \Psi_i \rangle|^2. \quad (1)$$

Here, ω_0 is the energy of the incident photons, ω_{if} is the transition energy between initial and final states, and the sum runs over all Cartesian components ρ and σ of the polarizability tensor $\hat{\alpha}_{\rho\sigma}$. In normal first-order Stokes scattering, the initial state is the electronic and vibrational ground state of the molecule (g_0) and the final state is the electronic ground state g_1 with one vibrational quantum in mode a . In Albrecht's theory, the respective matrix elements of the polarizability, $(\alpha_{\rho\sigma})_{g_0, g_1}$, read

$$(\alpha_{\rho\sigma})_{g_0, g_1} = A + B, \quad (2)$$

wherein the *Albrecht A-term* is given by^{42,43}

$$A = 2(\omega_a)^{3/2} \sum_e \Delta Q_a^e (\mu_{\rho'}^0)_{eg} (\mu_{\sigma'}^0)_{ge} \frac{\omega_{eg}^2 + \omega_0^2}{(\omega_{eg}^2 - \omega_0^2)^2} \quad (3)$$

(in atomic units). The sum runs over all electronically excited states. The quantities that enter this expression can be readily obtained by quantum-chemical methods: (i) ΔQ_a^e is the contribution of normal mode Q_a to the total (mass-weighted) change in the equilibrium geometry of the molecule upon electronic transition into the excited state e ; (ii) $(\mu_{\rho'}^0)_{eg}$ and $(\mu_{\sigma'}^0)_{ge}$ are the electric dipole matrix elements between the electronic ground and excited states (g and e respectively) at the ground-state equilibrium geometry; (iii) ω_{eg} denotes the transition energy between electronic ground and excited states at the ground-state equilibrium geometry; and (iv) ω_a stands for the vibrational energy quantum of mode a in the electronic ground state. This energy also enters into Eq. (1) ($\omega_{if} = \omega_a$) when calculating the intensity from the polarizabilities.

In the following, only the Albrecht A -terms will be considered. This is justified by the fact that, while in general B -term scattering cannot be neglected in the off-resonance regime, experimental Raman excitation profiles have demonstrated the dominance of A -term scattering for the considered vibrational modes and molecules.^{26,44,45} Furthermore, this restriction to the Albrecht A -terms permits to draw a more straightforward picture for the encountered mechanisms while, at the same time, satisfactorily reproducing experimental findings (*vide infra*).

The model presented above extends on the Ja -mode model¹⁹ in that (i) It takes more than one electronic excited state into account, which is important in the nonresonant regime. (ii) The ground- to excited-state distortion, i.e., the Ja mode, of the molecule is not constructed in a somewhat *ad hoc* manner (by changing the bond-length alternation from aromatic to quinoid) but rather calculated from *first-principles*. This not only yields a more accurate description of the ground- to excited-state distortion but also intrinsically takes the *end-group effects* of the finite oligomers fully into account.

The vibrational frequencies and normal coordinates have been calculated in the framework of density functional theory (DFT) at the respective equilibrium geometry. The modified Perdew and Wang exchange functional (mPW) was used⁴⁶ in conjunction with the Lee, Yang, and Parr (LYP) correlation energy functional.⁴⁷ A double- ζ contracted 4-31G** Gaussian basis set,⁴⁸⁻⁵¹ which contains one set of higher angular momentum polarization functions on each atom, was employed for all types of calculations. The vertical excitation energies, oscillator strengths, and displacements between ground and excited state equilibrium geometries of the molecules were calculated at the Hartree-Fock (HF) level, applying a configuration interaction scheme including only singly excited determinants (CIS) for excited-state properties.⁵² The CI-active space was scaled with the number of molecular orbitals (MOs) that can be derived from the doubly degenerate highest occupied MO (HOMO) and lowest unoccupied MO (LUMO) of benzene, the repeat unit in the OPPs.⁵³⁻⁵⁶ This leads to CI-active spaces ranging from four occupied and four unoccupied MOs in 2P to 6 and 6 for

P3P, 8 and 8 for P4P, 10 and 10 for P5P, and 12 and 12 for P6P. All these MOs have essentially π -character and the lowest excited states of the OPPs can be adequately described by single-electron excitations among them.

In order to investigate the influence of the inter-ring torsion angle on the Raman intensities, all the quantities mentioned above have been calculated at a series of fixed inter-ring torsion angles in the ground-state geometry of the molecules. Since this study aims at shedding light on the interplay between the molecular conformation and Raman intensities, at any given (fixed) value of the inter-ring torsion angle, the geometry of the molecule has been relaxed with the respective method (DFT or HF) first; the individual phenylene rings were forced to be fully planar. All inter-ring torsion angles were set to equal values. Since the present study also aims at providing guidelines for the interpretation of experiments conducted on solid-state samples,^{28-30,33,34} two adjacent inter-ring torsion angles were chosen to be of opposite sign.⁵⁷⁻⁵⁹

All calculations have been performed with the GAUSSIAN98 quantum-chemical program,⁶⁰ using tight convergence criteria for the self-consistent-field cycles, geometry optimization, frequency calculations, and the CIS scheme. GAUSSIAN98 also provides Raman intensities from static polarizabilities as a standard output in DFT frequency calculations, which will be compared to the results from the more complex model presented above. All calculated frequencies are reported unscaled; they are a direct output of the DFT calculations. All calculated spectra have been broadened with a Lorentzian peak-shape function with full width at half maximum is equal to 10 cm⁻¹ and are normalized to the highest peak. An incident laser wavelength of $\lambda_0 = 647.1$ nm (red line of a Krypton ion laser) has been assumed for the calculations unless otherwise stated.

III. RESULTS AND DISCUSSION

A. Dependence of the Raman polarizability on the number of excited states included in the sum-over-states expression

The Albrecht A -term [Eq. (3)] comprises a sum over all excited states (SOS) of the molecule. In order to limit the number of parameters for the subsequent interpretation of our results, it is useful to truncate this sum to a few dominant terms. In the series of investigated OPPs, the shortest oligomer, 2P, has the most well defined electronic structure due to the limited number of electrons. Therefore, it can serve as the model compound to identify important terms in the SOS. The CI-active space chosen for 2P comprises the four highest occupied MOs and the four lowest unoccupied MOs (*vide infra*), yielding a total of 16 excited states within the CIS scheme. Among these, four are polarized along the long molecular axis z (symmetry species $B_{1(u)}$). The considered Raman lines are also dominated by the polarizability tensor component $(\alpha_{zz})_{g0,g1_a}$ [see Eq. (1)].^{45,61} Consequently, only z -polarized electric dipole matrix elements $(\mu_z^0)_{ge}$ need to be taken into account in Eq. (3). Of the remaining four states, only three ($|1\rangle$, $|2\rangle$, and $|3\rangle$) have non-negligible oscillator strength. The dependence of I_{1280}/I_{1220} on the number of

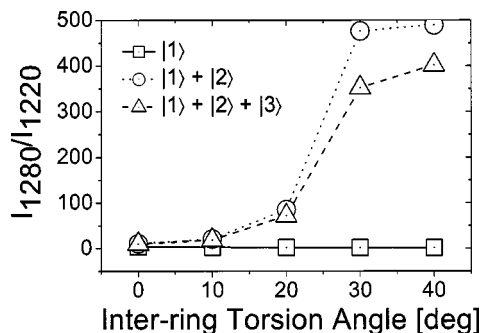


FIG. 2. Calculated intensity ratio I_{1280}/I_{1220} for biphenyl as a function of the interring torsion angle with one, two, and three excited electronic states taken into account in the sum-over-states expansion of the Albrecht A -terms.

included excited electronic states is shown in Fig. 2 as a function of the interring torsion angle. Interring torsion angles of more than 40° have not been considered in the present work, since OPPs do not assume equilibrium conformations with the dihedral angle between the phenylene rings being $>45^\circ$, even as isolated molecules in the gas phase.^{62–66} A truncation of the SOS expression in Eq. (3) after the lowest energy electronic excited state leads to a considerable error in the description of I_{1280}/I_{1220} in the nonresonant case, whereas the sum over $|1\rangle$ and $|2\rangle$ already reproduces the general trend quite well. Excited state $|3\rangle$ can be neglected to a first approximation.

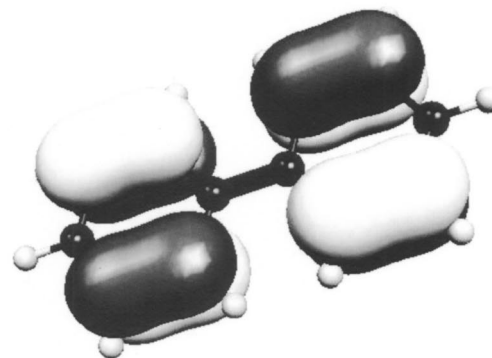
B. Nature of the excited states

The particular electronic structure of the OPPs can be exploited to further characterize the nature of the electronic excited states mentioned above. All MOs included in the CI-active space chosen for the description of electronic excited states in OPPs can be derived from the doubly degenerate HOMO and LUMO of benzene, the repeat unit in the OPPs.^{53–56} Consequently, there are four occupied and four unoccupied MOs of this particular nature in 2P, six in P3P, eight in P4P, ten in P5P, and 12 in P6P. These can be further divided into *delocalized* orbitals and *localized* orbitals.^{53–56,67} The former extend over the whole molecule with large electron density on the C atoms on the long molecular axis (*para* positions); thus, they are strongly influenced by conjugation (chain length and planarity). The localized orbitals have important contributions on the off-axis C atoms (*ortho* positions) and are thus far less susceptible to conjugation effects. In Fig. 3, the HOMO and HOMO-1 of 2P are shown as examples for delocalized and localized states, respectively.

The lowest energy excited state of 2P ($|1\rangle$) is dominated by a one-electron transition from the HOMO into the LUMO. Since both MOs are of a delocalized nature, this corresponds to a delocalized-delocalized transition (hereafter denoted as D -band). The second excited state ($|2\rangle$) corresponds to transitions from lower lying occupied localized MOs to higher lying unoccupied localized MOs. This localized-localized transition will be denoted as L band. The ordering of the MOs, their particular nature and the corresponding excited states can be tracked from 2P over all the oligomers on to the polymer.^{53,55} Although the total number of excited states increases upon increasing oligomer length



(a)HOMO



(b)HOMO-1

FIG. 3. Illustration of the delocalization of the HOMO of biphenyl (a) over the long molecular axis and the localization of the HOMO-1 (b) on the off-axis carbon atoms.

(and correspondingly increasing CI-active space), only one strongly allowed D band and one strongly allowed L band are observed in oligomers of any length.

We thus chose to restrict the SOS description of the Raman intensities to these two bands for all investigated oligomers up to six repeat units (P6P). This truncation not only keeps the computational effort at an acceptable level but also limits the number of parameters for the subsequent interpretation of our results.

In Fig. 4, the transition energies and the electric dipole matrix elements for the D and L bands are plotted as a function of oligomer length and interring torsion angle.⁶⁸ While the D bands are strongly influenced by the effective conjugation length (determined by the number of repeat units and the planarity), the effect on the L bands is much weaker. This is consistent with the delocalized/localized character of the MOs taking part in the respective transitions. The trends predicted by the CIS method are found to be in good agreement with experiment, while the transition energies are somewhat overestimated⁶⁹ (this is partly inherent to the method, partly due to the relatively small basis set chosen in the present work, and partly due to the neglect of solvent effects).⁷⁰

Among all the parameters needed to evaluate the Raman intensities within Albrecht's theory [$\omega_a, \Delta Q_a^e, (\mu_\rho)_{eg}^0, \omega_{eg}$], the values for the transition energies and electric transition dipole moments (Fig. 4) enter with the highest powers (qua-

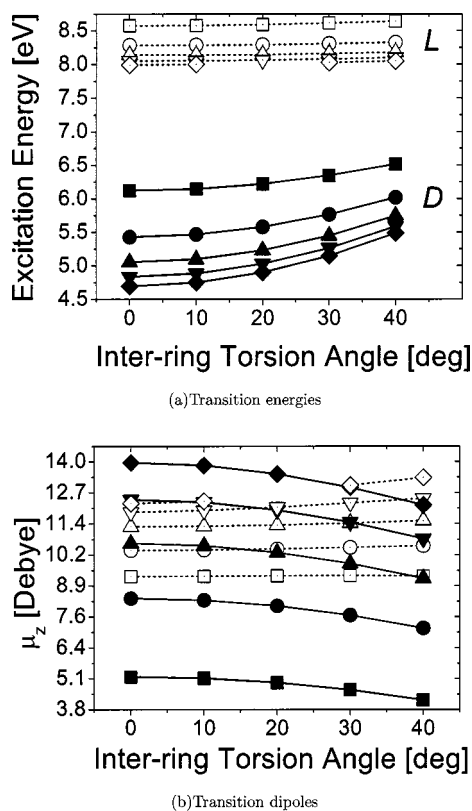


FIG. 4. Transition energies (a) and electric transition dipole matrix elements (b) for the *D* bands (full symbols) and *L* bands (empty symbols) of 2P (square), P3P (circle), P4P (up triangle), P5P (down triangle), and P6P (diamond) (Ref. 68).

dratic vs linear) into the expression for the Raman polarizability [Eq. (3)] of the two modes. Hence, the evolution of these two quantities with chain length and interring torsion angle dominates the dependence of the respective Raman polarizabilities on conjugation-related parameters.

C. Relative intensity and oligomer length

First, we will discuss the evolution of the intensity ratio I_{1280}/I_{1220} with chain length. An interring torsion angle of 10° has been assumed for all oligomer lengths in the calculations, since this value has been determined experimentally for OPPs in crystalline environment at room temperature.^{57–59}

The atomic displacements associated with the 1220 cm^{-1} mode (Fig. 1) more closely resemble the geometry distortion that the molecule undergoes upon transition into the *D* state than they resemble the geometry distortion upon excitation into the *L* state. This is reflected by the fact that the projection of the former distortion onto the 1220 cm^{-1} normal coordinate, ΔQ_{1220}^D , is larger than that of the latter, ΔQ_{1220}^L (see Table I), for oligomer lengths 3 and longer.⁷¹ Consequently, the Raman polarizability of the 1220 cm^{-1} mode is predominantly related to the *D* band, i.e., its intensity is strongly coupled to the magnitude of the transition energies and transition dipoles of the *D* band. These quantities are highly sensitive to chain length: the transition energies decrease upon increasing chain length while the transition dipole moments increase (see Fig. 4). Thus, one can expect the

TABLE I. Projections (in $\sqrt{\text{amu}} \text{ \AA}$) of the equilibrium geometry distortions upon transition from the electronic ground state into the *D* and *L* states onto the normal coordinates of the 1220 and 1280 cm^{-1} modes for biphenyl (2P), *p*-terphenyl (P3P), *p*-quaterphenyl (P4P), *p*-quinquephenyl (P5P), and *p*-sexiphenyl (P6P). Values are given for an interring torsion angle of 10° (see text for details) (Refs. 71 and 74). For the projections onto the *D* states, also the percentage is given (in brackets) of how much the respective modes contribute to the total ground- to excited-state distortion.

Molecule	1220 (cm^{-1})		1280 (cm^{-1})	
	<i>D</i> state	<i>L</i> state	<i>D</i> state	<i>L</i> state
2P	0.10 (9.4%)	-0.12	0.16 (14.9%)	0.10
P3P	0.18 (14.8%)	-0.10	0.11 (9.1%)	0.15
P4P	0.18 (10.8)	-0.10	0.08 (5.1%)	0.17
P5P	0.17 (8.5%)	-0.11	0.11 (5.2%)	0.17
P6P	0.17 (6.8%)	-0.12	0.10 (4.0%)	0.19

1220 cm^{-1} mode to be strongly *conjugation enhanced*.^{72,73}

In contrast, the atomic displacements associated with the 1280 cm^{-1} mode show more similarity to the geometry distortion that the molecule undergoes upon transition into the *L* state (see Table I)⁷⁴ for low interring torsion angles (see the following section). Consequently, since the transition energies and transition dipoles associated with the *L* band are rather insensitive to chain length (see Fig. 4), the influence from the more conjugation enhanced *D* band on the intensity of the 1280 cm^{-1} mode is less pronounced.

In addition, for the 1280 cm^{-1} mode, the projections ΔQ_{1280}^D and ΔQ_{1280}^L have the same sign, while for the 1220 cm^{-1} mode ΔQ_{1220}^D and ΔQ_{1220}^L are of opposite sign (see Table I). Accordingly, the two respective terms in the SOS expression for the Raman polarizability [summed over in Eq. (3) for $e=D,L$] are of the same sign for the 1280 cm^{-1} mode, while they are of opposite sign for the 1220 cm^{-1} mode (see Fig. 5). Thus, in the case of the 1280 cm^{-1} mode, a less conjugation enhanced term (contribution from the *L* state) is *added* to a more conjugation enhanced term (contribution from the *D* state). This lessens the relative change of the sum of the two terms, I_{1280} , upon increasing chain length. For the 1220 cm^{-1} mode, on the other hand, a fairly constant term (contribution from the *L* state) is *subtracted* from a strongly conjugation enhanced term (contribution from the *D* state), which enlarges the relative change of I_{1220} , the sum of the two terms [Eq. (3)].

Altogether, this leads to an overall decrease of I_{1280}/I_{1220} upon increasing oligomer length, which is fully consistent with the experimental results shown in Fig. 6, where our calculated Raman spectra are compared to measurements on polycrystalline powders of OPPs. Good quantitative agreement is found. In contrast, the Raman intensities calculated from static (DFT) polarizabilities (represented by thin solid lines in Fig. 6), while providing the correct trends, severely underestimate (<1.0) the absolute values of I_{1280}/I_{1220} for oligomers longer than 2P. For the latter, the two lines coincide.

The percentage values given in brackets in Table I show how much the respective mode contributes to the total (HF/CIS calculated) ground- to first excited-state distortion. If

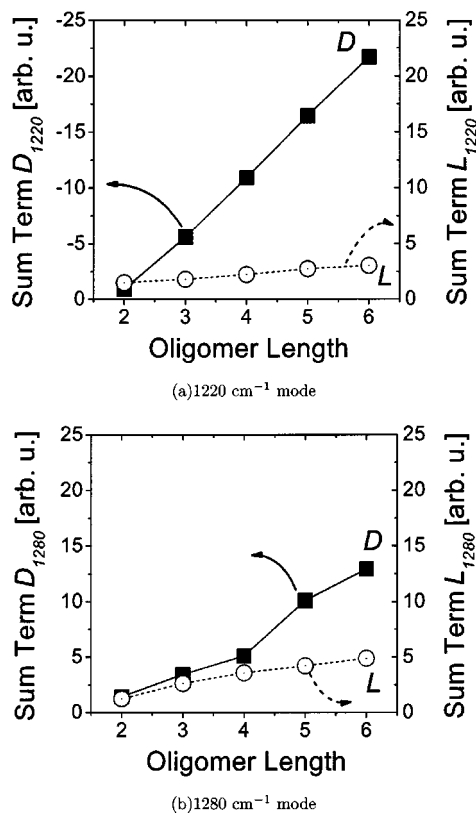


FIG. 5. Evolution of the dominant terms in the SOS expansion of the Raman polarizability [Eq. (3)] with oligomer length for the 1220 cm^{-1} mode (a) and the 1280 cm^{-1} mode (b) (Ref. 74). The contribution arising from coupling to the D band is shown in solid squares, the contribution from coupling to the L state in open circles.

one took the Ja -mode¹⁹ to be the actual ground- to first excited-state distortion rather than a constructed bond-length alternation mode (aromatic to quinoid), these numbers would

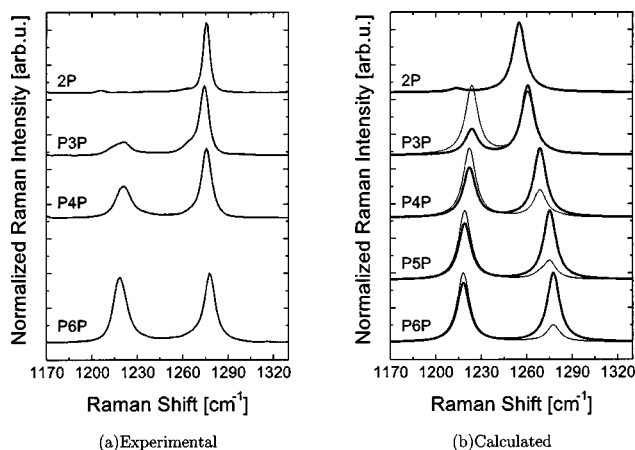


FIG. 6. Experimental solid-state (a) and calculated (b) detail of the Raman spectra of 2P, P3P, P4P, P5P (calculated only), and P6P in the $1200\text{--}1300\text{ cm}^{-1}$ region; the calculated spectra are based on interring torsion angles of 10° . The thick solid lines in (b) represent the results obtained by the model presented in this work; the thin solid lines are directly obtained from static polarizabilities routinely provided by quantum-chemical DFT frequency calculations. In the case of 2P, the two calculated spectra coincide. Both the experimental and calculated spectra are normalized to the respective higher peak [1280 cm^{-1} in the case of (a) and thick solid lines in (b), 1220 cm^{-1} in the case of thin solid lines in (b)].

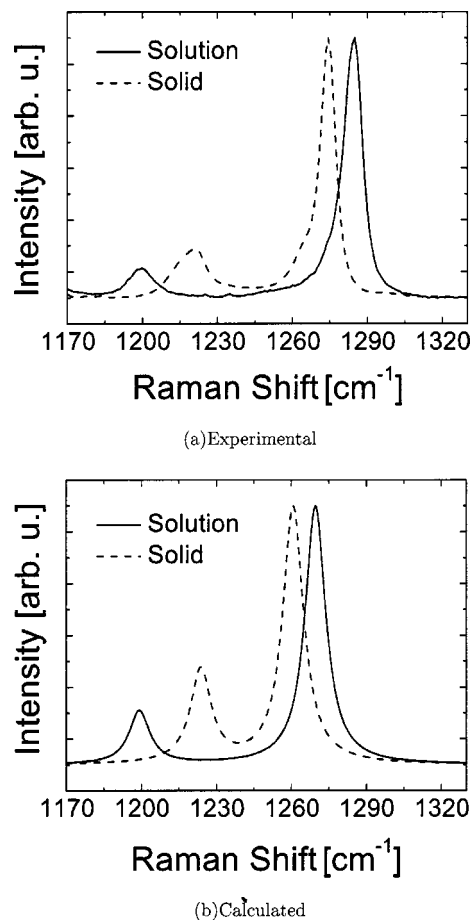


FIG. 7. Experimental (a) and calculated (b) Raman spectra of P3P in the crystal (dashed lines) and in solution (solid lines) in the $1200\text{--}1300\text{ cm}^{-1}$ region; the calculated spectra are based on interring torsion angles of 10° (crystal) and 30° (solution).

correspond to (relative) Raman intensities within the Ja -mode model.¹⁹ Again, the trend is reproduced while the absolute values for I_{1280}/I_{1220} are not.

D. Relative intensity and planarity

In addition to oligomer length, the dihedral angle between adjacent phenyl rings influences the effective conjugation of the π -electron system. While the interring torsion angle of OPPs has been found to be ca. 10° in the crystalline phase at room temperature^{57–59} (*vide supra*), it has been determined to be ca. 30° in solution.^{75–78} In Fig. 7, the experimental and calculated Raman spectra are plotted for P3P in the solid state and in solution. For this relatively small system where the torsion is well established, they consistently show that I_{1280}/I_{1220} decreases upon planarization of the molecules, as suggested in Refs. 28–30, 33, and 34.

In order to understand this behavior, it is again necessary to consider the contributions arising from the D and L bands and their variation with the interring torsion angle. The transition energies of the D band decrease upon planarization of the OPPs and the electric transition dipoles increase (see Fig. 4), while the transition energies and dipoles of the L band are much less susceptible to changes in the effective conjugation induced by the coupling between the phenylene rings. For

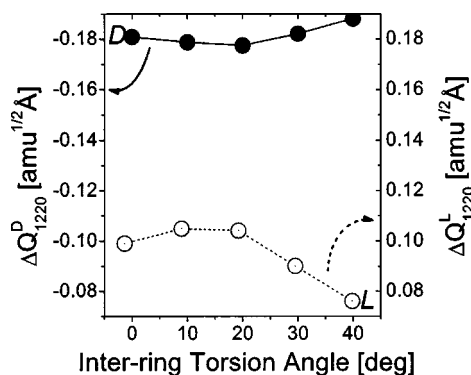
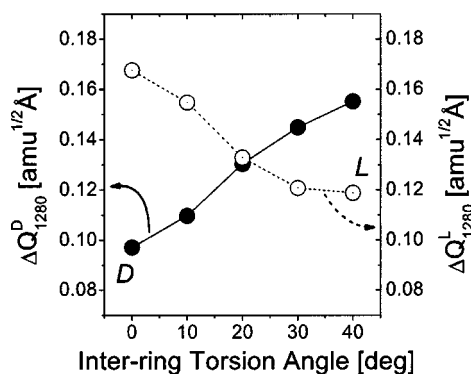
(a) 1220 cm⁻¹ mode(b) 1280 cm⁻¹ mode

FIG. 8. Mass-weighted projection of the interstate distortions upon exciting *p*-terphenyl into the *D* and *L* state onto the normal coordinates of the 1220 cm⁻¹ (a) and 1280 cm⁻¹ (b) modes.

the sake of clarity, the remaining parameters will be discussed in the following for P3P; all longer oligomers behave identically.

The values of the projection of the interstate distortions upon exciting the molecule into the *D* and *L* states onto the normal coordinates of the 1220 and 1280 cm⁻¹ mode are shown in Fig. 8 as a function of the interring torsion angle. As mentioned above, ΔQ^D is always larger than ΔQ^L for the 1220 cm⁻¹ mode while for the 1280 cm⁻¹ mode, this is true only for large interring torsion angles; a crossover is observed at $\sim 20^\circ$ so that for more planar conformers, the 1280 cm⁻¹ mode is dominated by the *L* band. In addition, we recall that ΔQ_{1220}^D and ΔQ_{1220}^L are of opposite sign, while ΔQ_{1280}^D and ΔQ_{1280}^L have the same sign.

The interring torsion angle dependence of the intensity of the 1220 cm⁻¹ mode can be rationalized in a straightforward manner: It is dominated by (virtual) transitions to the *D* band (Fig. 8) and therefore strongly conjugation enhanced upon planarization (see Fig. 9). The strong torsion angle dependence of the intensity of the 1220 cm⁻¹ mode is further enhanced by the fact that *D*- and *L*-band contributions (shown in Fig. 9) enter the SOS expression [Eq. (3)] with opposite signs.

This (partial) cancellation of *D* and *L* terms is more pronounced in 2P and thus responsible for the vanishing intensity of the 1220 cm⁻¹ mode, especially at high interring torsion angles (Fig. 2). In fact, this effect even dominates over

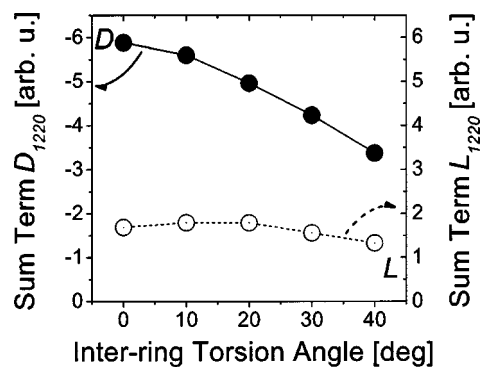
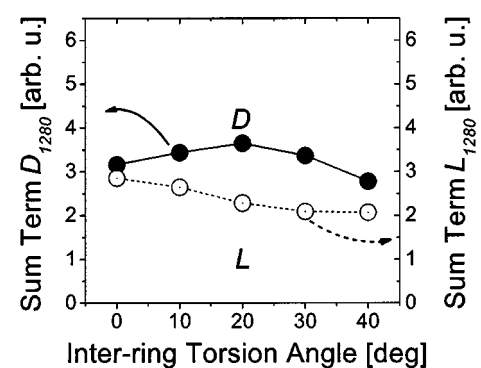
(a) 1220 cm⁻¹ mode(b) 1280 cm⁻¹ mode

FIG. 9. Interring torsion angle dependence of the dominant terms in the SOS expansion of the Raman polarizability [Eq. (3)] for the 1220 cm⁻¹ mode (a) and the 1280 cm⁻¹ mode (b) in *p*-terphenyl. The contribution arising from coupling to the *D* band is shown in solid squares, the contribution from coupling to the *L* state in open circles.

the relative weights (ΔQ^D vs ΔQ^L) of the two sum terms in 2P, which are actually inverted with respect to the longer oligomers (see Table I).

The situation is somewhat more complex for the 1280 cm⁻¹ mode. At lower torsion angles, the mode intensity is dominated by the *L* band (see Fig. 8) which is much less susceptible to varying conjugation (see Fig. 4). At higher interring torsion angles, the *D*-band gains a more dominant character also for the 1280 cm⁻¹ mode (Fig. 8); the effect is, however, largely compensated by the decreasing transition dipoles and increasing excitation energies of the *D* band (Fig. 4). This results in both the *D*- and *L*-state contributions in the SOS expression to show a less pronounced torsion angle dependence (Fig. 9). Consequently, the sum of the two terms (of equal sign), I_{1280} , shows a relatively less pronounced interring torsion angle dependence as compared to I_{1220} .

The resulting calculated dependence of the relative intensity I_{1280}/I_{1220} on the interring torsion angle is presented in Fig. 10 for oligomers containing from three to six repeat units⁶⁸ (the data for 2P is contained in Fig. 2). It is observed that the I_{1280}/I_{1220} ratio decreases with decreasing torsion angle; in addition, the sensitivity of I_{1280}/I_{1220} on the planarity of the molecules decreases upon increasing oligomer length. This is in accordance with previously published experimental data.^{28,29,33,34} For P6P, the few-state model pre-

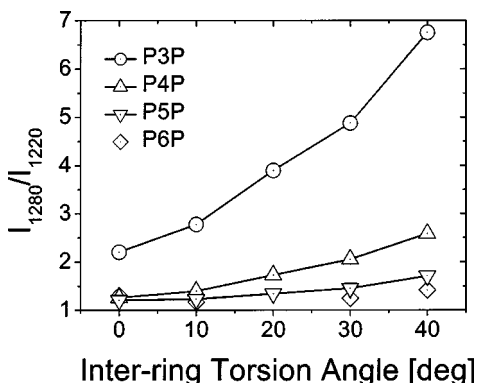


FIG. 10. Calculated intensity ratio I_{1280}/I_{1220} for the OPPs as a function of the interring torsion angle (Ref. 68).

sented in this work shows the weakest trend and I_{1280}/I_{1220} is actually slightly higher at 0° than it is at 10° .⁷⁹

E. Relative intensity and excitation wavelength

In Fig. 11(a), the experimental Raman spectrum of P3P in CH_2Cl_2 solution is shown as recorded with a laser wavelength of 647.1 nm (Krypton ion laser) and with the 457.9 nm line of an argon ion laser. Realigning the optical setup for the new laser source resulted in a small shift in the experimental Raman frequencies, which obviously cannot appear in the calculations. For better comparison, the experimental Raman spectra have therefore been horizontally

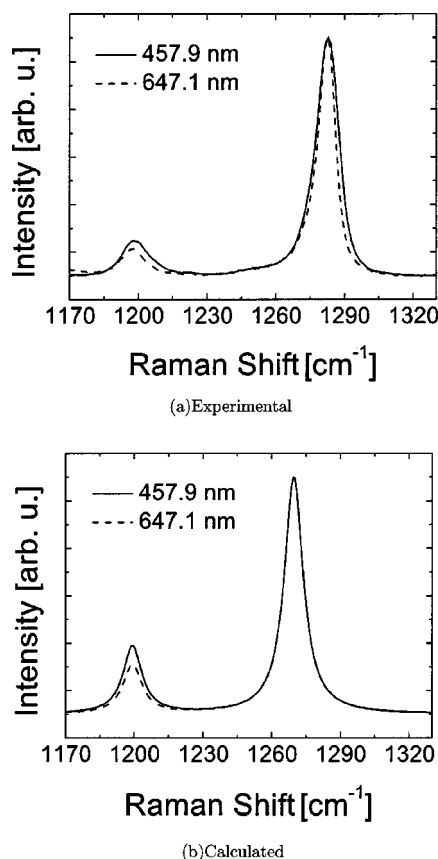


FIG. 11. Experimental (a) and calculated (b) detail of the Raman spectra of P3P in CH_2Cl_2 solution recorded (calculated) for a laser excitation wavelength of 457.9 nm (solid lines) and 647.1 nm (dashed lines).

shifted (within the experimental error of $\pm 1 \text{ cm}^{-1}$) until the two (experimental) 1280 cm^{-1} lines came to lie on top of each other. The calculated frequencies are reported unscaled. All spectra are normalized to the 1280 cm^{-1} peak.

For the 1220 cm^{-1} mode, the contribution to the Raman intensity stemming from coupling to the D state is more pronounced than for the 1280 cm^{-1} mode. Consequently, as the exciting laser line approaches resonance with the lower energy D -band, the 1220 cm^{-1} mode is more strongly pre-resonance enhanced than the 1280 cm^{-1} mode. This results in an overall decrease (ca. 21%) of the intensity ratio I_{1280}/I_{1220} upon increasing the excitation energy, which is fully consistent with our theoretical results (decrease by ca. 28%) shown in Fig. 11(b).

For other oligomer lengths, a similar behavior has been observed experimentally.^{18,26,28} We expect the same interpretation as for P3P to hold in these cases.

IV. CONCLUSIONS

We have investigated the interplay between conjugation and the intensity of two Raman active modes at 1220 and 1280 cm^{-1} in oligo(*para*-phenylene)s. Applying Albrecht's theory, we show that the 1220 cm^{-1} mode draws its intensity mainly from a (virtual) transition into the lowest excited electronic state. This state can be described by transitions from delocalized occupied MOs into delocalized unoccupied MOs, which are very sensitive to conjugation (affected by chain length and planarity). As a consequence, the 1220 cm^{-1} mode is very sensitive to these parameters, experiencing strong conjugation enhancement. A more complex interplay between the vibrational coupling to the delocalized and localized electronic states leads to a less pronounced conjugation enhancement of the 1280 cm^{-1} mode.

Overall, the intensity ratio I_{1280}/I_{1220} decreases upon increasing the effective conjugation length which can be achieved either by increasing the number of repeat units in the oligomer or by reducing the interring torsion angle. In addition, the 1220 cm^{-1} mode is more strongly pre-resonance enhanced than the 1280 cm^{-1} mode.

The *first-principles*, Albrecht's theory calculations presented in this work are in good quantitative agreement with the experimental findings reported here and in the literature. Moreover, they allow to trace the observed effects down to their microscopic (quantum mechanical) origin and to the distinct nature of the MOs and the excited states in the oligo(*para*-phenylene)s. Thus, they represent a sound theoretical foundation for linking the intensity ratio of the 1220 and 1280 cm^{-1} Raman lines to the degree of conjugation in oligo(*para*-phenylene)s.

ACKNOWLEDGMENTS

The work in Graz is supported by the Austrian Fonds zur Förderung der Wissenschaftlichen Forschung (Project No. P14237-PHY, Project No. P14170-TPH, and Spezialforschungsbereich Elektroaktive Stoffe). The work at Georgia Tech is partly supported by the US National Science Foundation (Grant No. CHE-0343412 and STC program Award No. DMR-0120967).

- ¹R. R. Chance, D. S. Boudreaux, J. L. Bredas, and R. Silbey, in *Handbook of Conducting Polymers*, edited by T. J. Skotheim (Marcel Dekker, New York, 1986), Vol. 2, p. 825.
- ²J. L. Bredas, in *Handbook of Conducting Polymers*, Ref. 1, Vol. 2, p. 859.
- ³R. L. Elsenbaumer and L. W. Shacklette in *Handbook of Conducting Polymers*, Ref. 1, Vol. 2, p. 213.
- ⁴C. Kallinger, M. Hilmer, A. Haugeneder *et al.*, *Adv. Mater. (Weinheim, Ger.)* **10**, 920 (1998).
- ⁵G. Grem, G. Leditzky, B. Ulrich, and G. Leising, *Adv. Mater. (Weinheim, Ger.)* **4**, 36 (1992).
- ⁶M. T. Bernius, M. Inbasekaran, J. O'Brien, and W. Wu, *Adv. Mater. (Weinheim, Ger.)* **12**, 1737 (2000).
- ⁷A. Corney, J. Manners, and C. E. Webb, *Opt. Commun.* **31**, 354 (1979).
- ⁸V. S. Zuev, O. A. Logunov, V. Savinov-Yu, A. V. Startsev, and Y. Y. Stoilov, *Appl. Phys.* **17**, 321 (1978).
- ⁹J. L. Nogues, S. Majewski, J. K. Walker, M. Bowen, R. Wojcik, and W. V. Moreshead, *J. Am. Ceram. Soc.* **71**, 1159 (1988).
- ¹⁰R. Tousey and I. Limansky, *Appl. Opt.* **11**, 1025 (1972).
- ¹¹S. Tasch, C. Brandstätter, F. Meghdadi, G. Leising, G. Froyer, and L. Athouël, *Adv. Mater. (Weinheim, Ger.)* **9**, 33 (1997).
- ¹²M. Era, T. Tsutsui, and S. Saito, *Appl. Phys. Lett.* **67**, 2436 (1996).
- ¹³D. J. Gundlach, Y.-Y. Lin, T. N. Jackson, and D. G. Schlom, *Appl. Phys. Lett.* **71**, 3853 (1997).
- ¹⁴L. Cuff and M. Kertesz, *Macromolecules* **27**, 762 (1994).
- ¹⁵L. Cuff and M. Kertesz, *J. Phys. Chem.* **98**, 12223 (1994).
- ¹⁶L. Cuff, M. Kertesz, U. Scherf, and K. Müllen, *Synth. Met.* **69**, 683 (1994).
- ¹⁷S. Krichene, J. P. Buisson, and S. Lefrant, *Synth. Met.* **17**, 589 (1987).
- ¹⁸J. P. Buisson, S. Krichene, and S. Lefrant, *Synth. Met.* **21**, 229 (1987).
- ¹⁹C. Castiglioni, M. Gussoni, and G. Zerbi, *Synth. Met.* **29**, E1 (1989).
- ²⁰J. Soto, V. Hernandez, and J. T. Lopez-Navarette, *Synth. Met.* **51**, 229 (1992).
- ²¹A. Marucci, A. Pimenta, S. D. M. Brown, M. J. Matthews, M. S. Dresselhaus, and M. Endo, *J. Mater. Res.* **14**, 3447 (1999).
- ²²Y. Furukawa, *J. Phys. Chem.* **100**, 15644 (1996).
- ²³Y. Furukawa, H. Ohtsuka, and M. Tasumi, *Synth. Met.* **55–57**, 516 (1993).
- ²⁴G. Zannoni and G. Zerbi, *J. Chem. Phys. Lett.* **82**, 31 (1985).
- ²⁵G. Heimel, D. Somitsch, P. Knoll, and E. Zojer, *J. Chem. Phys.* **116**, 10921 (2002).
- ²⁶H. Ohtsuka, Y. Furukawa, and M. Tasumi, *Spectrochim. Acta, Part A* **49**, 731 (1993).
- ²⁷G. Leising, T. Verdon, G. Louarn, and S. Lefrant, *Synth. Met.* **41–43**, 279 (1991).
- ²⁸S. Guha, W. Graupner, R. Resel, M. Chandrasekhar, H. R. Chandrasekhar, R. Glaser, and G. Leising, *J. Phys. Chem. A* **105**, 6203 (2001).
- ²⁹S. Guha, W. Graupner, R. Resel, M. Chandrasekhar, H. R. Chandrasekhar, R. Glaser, and G. Leising, *Phys. Rev. Lett.* **82**, 3625 (1999).
- ³⁰M. Chandrasekhar, S. Guha, and W. Graupner, *Adv. Mater. (Weinheim, Ger.)* **13**, 613 (2001).
- ³¹P. Knoll, R. Singer, and W. Kiefer, *Appl. Spectrosc.* **44**, 1990 (1990).
- ³²M. J. Frisch, Y. Yamaguchi, J. F. Gaw, H. F. Schaefer, and J. S. Binkley, *J. Chem. Phys.* **84**, 531 (1986).
- ³³G. Heimel, P. Puschnig, Q. Cai, C. Martin, E. Zojer, W. Graupner, M. Chandrasekhar, H. R. Chandrasekhar, C. Ambrosch-Draxl, and G. Leising, *Synth. Met.* **116**, 163 (2001).
- ³⁴G. Heimel, Q. Cai, C. Martin *et al.*, *Synth. Met.* **119**, 371 (2001).
- ³⁵M. Rumi and G. Zerbi, *Chem. Phys.* **242**, 123 (1999).
- ³⁶J. Kürti and H. Kuzmany, *Phys. Rev. B* **44**, 597 (1991).
- ³⁷E. Ehrenfreund, Z. Vardeny, O. Brafman, and B. Horovitz, *Phys. Rev. B* **36**, 1535 (1987).
- ³⁸E. Mulazzi, A. Ripamonti, L. Athouël, J. Wery, and S. Lefrant, *Phys. Rev. B* **65**, 085204 (2002).
- ³⁹E. Mulazzi, A. Ripamonti, J. Wery, B. Dulieu, and S. Lefrant, *Phys. Rev. B* **60**, 16519 (1999).
- ⁴⁰S. Matsumura, *Thin Solid Films* **306**, 17 (1997).
- ⁴¹C. Castiglioni, J. T. Lopez-Navarette, G. Zerbi, and M. Gussoni, *Solid State Commun.* **65**, 625 (1988).
- ⁴²A. C. Albrecht, *J. Chem. Phys.* **34**, 1476 (1961).
- ⁴³A. C. Albrecht and M. C. Hutley, *J. Chem. Phys.* **55**, 4438 (1971).
- ⁴⁴E. D. Schmid and R. D. Topsom, *J. Am. Chem. Soc.* **103**, 1628 (1981).
- ⁴⁵A. Bree, R. Zwarich, and C. Taliani, *Chem. Phys.* **70**, 257 (1982).
- ⁴⁶C. Adamo and V. Barone, *J. Chem. Phys.* **108**, 664 (1998).
- ⁴⁷C. Lee, W. Yang, and R. G. Parr, *Phys. Rev. B* **37**, 785 (1988).
- ⁴⁸R. Ditchfield, W. J. Hehre, and J. A. Pople, *J. Chem. Phys.* **54**, 724 (1971).
- ⁴⁹M. J. Frisch and J. A. Pople, *J. Chem. Phys.* **80**, 3265 (1984).
- ⁵⁰W. J. Pietro, M. M. Francl, W. J. Hehre, D. J. DeFrees, J. A. Pople, and J. S. Binkley, *J. Am. Chem. Soc.* **104**, 5039 (1982).
- ⁵¹K. D. Dobbs and W. J. Hehre, *J. Comput. Chem.* **7**, 359 (1986).
- ⁵²J. B. Foresman, M. Head-Gordon, J. A. Pople, and M. J. Frisch, *J. Phys. Chem.* **96**, 135 (1992).
- ⁵³J. L. Brédas, R. R. Chance, R. Silbey, G. Nicolas, and P. Durand, *J. Chem. Phys.* **77**, 371 (1982).
- ⁵⁴M. J. Rice and Y. N. Gartstein, *Phys. Rev. Lett.* **73**, 2504 (1994).
- ⁵⁵P. Puschnig and C. Ambrosch-Draxl, *Phys. Rev. B* **60**, 7891 (1999).
- ⁵⁶M. Rubio, M. Merchán, E. Ortí, and B. O. Roos, *Chem. Phys. Lett.* **234**, 373 (1995).
- ⁵⁷H. M. Rietveld, E. N. Maslen, and C. J. B. Clews, *Acta Crystallogr., Sect. B: Struct. Crystallogr. Cryst. Chem.* **26**, 693 (1970).
- ⁵⁸J. L. Baudour, *Acta Crystallogr., Sect. B: Struct. Crystallogr. Cryst. Chem.* **47**, 935 (1991).
- ⁵⁹J. L. Baudour and H. Cailleau, *Acta Crystallogr., Sect. B: Struct. Crystallogr. Cryst. Chem.* **33**, 1773 (1977).
- ⁶⁰M. J. Frisch, G. W. Trucks, H. B. Schlegl *et al.*, GAUSSIAN98, Revision A.11, Gaussian, Inc., Pittsburgh PA, 2001.
- ⁶¹A. Bree, C. Y. Pang, and L. Rabenck, *Spectrochim. Acta, Part A* **27**, 1293 (1971).
- ⁶²O. Bastiansen, *Acta Chem. Scand.* (1947-1973) **3**, 408 (1949).
- ⁶³A. Almenningen, O. Bastiansen, L. Fernholt, B. N. Cyvin, S. J. Cyvin, and S. Samdal, *J. Mol. Struct.* **128**, 59 (1985).
- ⁶⁴S. Tsuzuki, T. Uchamaru, K. Matsumura, M. Mikami, and K. Tanabe, *J. Chem. Phys.* **110**, 2858 (1999).
- ⁶⁵J. C. Sancho-García, J. L. Brédas, and J. Cornil, *Chem. Phys. Lett.* **377**, 63 (2003).
- ⁶⁶A. Pogantsch, G. Heimel, and E. Zojer, *J. Chem. Phys.* **117**, 5921 (2002).
- ⁶⁷A. Köhler, D. A. dos Santos, D. Beljonne *et al.*, *Nature (London)* **392**, 903 (1998).
- ⁶⁸For P6P at an interring torsion angle of 20°, a otherwise dark state comes into resonance with the *L* band, shifting its energy and drawing away oscillator strength. Therefore, no values are reported for P6P at 20°.
- ⁶⁹N. I. Nijegorodov, W. S. Downey, and M. B. Danailov, *Spectrochim. Acta, Part A* **56**, 783 (2000).
- ⁷⁰J. Gierschner, H.-G. Mack, L. Lüer, and D. Oelkrug, *J. Chem. Phys.* **116**, 8596 (2002).
- ⁷¹Lacking central, *para*-substituted phenylene rings, 2P behaves differently than the longer OPPs in that the normal mode displacement patterns are not yet fully developed and end-group effects dominate. Both rings can be considered as end groups in this context.
- ⁷²E. D. Schmid and B. Brosa, *J. Chem. Phys.* **56**, 6267 (1972).
- ⁷³E. D. Schmid and B. Brosa, *J. Chem. Phys.* **58**, 3871 (1973).
- ⁷⁴The presence of two inequivalent aromatic rings in P4P and P5P (three in P6P) leads to a splitting of both 1220 and 1280 cm⁻¹ modes. While one mode is still dominant, all contribute to the total intensity of the spectral features at 1220 and 1280 cm⁻¹. Consequently, they have been taken into account when analyzing the *I*₁₂₈₀/*I*₁₂₂₀ ratio. This has proven most important in the case of P4P.
- ⁷⁵R. M. Barrett and D. Steele, *J. Mol. Struct.* **11**, 105 (1972).
- ⁷⁶V. J. Eaton and D. Steele, *J. Chem. Soc., Faraday Trans. 2* **69**, 1601 (1973).
- ⁷⁷M. Akiyama, *Spectrochim. Acta, Part A* **40**, 367 (1984).
- ⁷⁸A. Ghanem, L. Bokobza, C. Noel, and B. Marchon, *J. Mol. Struct.* **159**, 47 (1987).
- ⁷⁹Taking more excited states into account in the SOS expansion for the Raman polarizability [Eq. (3)] is expected to increase the accuracy of the calculations. However, the interpretation of the computed intensities and consequently of the experimental trends would rapidly become less straightforward.